

# A Simple Linear Model to Aid in Analyses of the $\beta$ Pictoris Moving Group

Josina O. do Nascimento  
Observatório Nacional  
Rua General José Cristino, 77  
20921-400 Rio de Janeiro - RJ, Brazil

Valmir C. Barbosa\*  
Programa de Engenharia de Sistemas e Computação, COPPE  
Universidade Federal do Rio de Janeiro  
Centro de Tecnologia, Sala H-319  
21941-914 Rio de Janeiro - RJ, Brazil

## Abstract

We build a four-dimensional linear model of object membership in the  $\beta$  Pictoris moving group (BPMG), using two nested applications of Principal Component Analysis (PCA) to high-quality data on about 1.5 million objects. These data contain the objects' galactic space velocities and also their *Gaia*  $G$  magnitudes. Through PCA, they ultimately result in a four-dimensional straight line, referred to as PC 1', about which both the bona fide members used to obtain the straight line and the candidate members used to test the model congregate at generally small distances. Our bona fide members come from a recent, *Gaia* DR2-based compilation. Most candidate members are from a compilation from 2017. Using a standard procedure to flag groups of outliers in data sets, we argue that flagging the few possible outliers we identified on account of distances to PC 1' is consistent with the nature of the candidate members in use. The spatial and kinematic measurements that backed their inclusion in the 2017 compilation were of course from before the availability of data from the *Gaia* mission. Moreover, their radial velocities at the time were either unknown or estimated somewhat unreliably. We propose that PC 1' be added to the tool set for BPMG analyses and potentially extended to other young stellar moving groups.

**Keywords:**  $\beta$  Pictoris moving group, Data analysis in astronomy.

---

\*Corresponding author (valmir@cos.ufrj.br).

# 1 Introduction

Of all the young stellar moving groups discovered and studied to date, the  $\beta$  Pictoris moving group (BPMG) [1] seems to offer the most tantalizing possibilities for research on planet formation and exoplanets. Not only is it closest to Earth, but also the star that gives BPMG its name has two confirmed planets orbiting it [2, 3]. These characteristics have motivated substantial effort in the last two to three decades to discover the group’s full suite of members. To the best of our knowledge, the most complete assessment of the BPMG membership dating from before the availability of data from the *Gaia* mission is to be found in [4]. This was soon followed by further comprehensive studies (cf., e.g., [5, 6]), with [5] already incorporating data from *Gaia* DR1 and subsequently undergoing updates as further data releases were made available.

The research underpinning studies such as these is based on spatial, kinematic, photometric, and several other types of measurement, the kinematic part comprising the usual galactic space velocities, viz.,  $U$ ,  $V$ , and  $W$ . The focus on these velocities has been widespread since relatively early on (cf., e.g., [7–9]), since a moving group’s members tend to cluster together in three-dimensional velocity space. This is always important information, something to be taken into account when looking to confirm new members, though checking the membership status of a new candidate based on such clusters must necessarily grapple with criteria from cluster analysis that tend to be ill defined [10].

Here we demonstrate that, by bringing in a fourth dimension to the data space, a new perspective is gained that can assist in the task of determining cluster membership by essentially requiring distances from points to a straight line in four-dimensional space to be calculated. With these distances available for all objects of interest (bona fide group members as well as candidate members), outliers can be flagged for further consideration on the basis of how such distances are distributed. Though in our initial trials with the data we observed this strategy to make sense for more than one choice of fourth dimension and more than one moving group, in this paper we deal exclusively with the fourth dimension being given by the *Gaia*  $G$  magnitude [11] and with the BPMG.

The possibility of running a straight line through such a four-dimensional representation of a proposed BPMG membership becomes evident as one examines any of the three two-dimensional plots involving dimension  $G$  ( $G \times U$ , etc.). However, pinning the line down through some generalization of simple linear regression to more than two dimensions would be fraught with difficult decisions, including deciding which variables to take as independent, something that already plagues the two-dimensional case in several domains. Our analysis in this work takes a longer, though still simple, route.

Aiming to make the representation of the data independent of measurement units and also amenable to visualization in a greater number of two-dimensional plots (six rather than three), we work on standardized versions of  $U$ ,  $V$ ,  $W$ ,  $G$  (i.e., versions whose means equal 0 and standard deviations equal 1) and moreover rotate the resulting data in such a way that they become represented by uncorrelated coordinates. Such rotation results from the well-known method of

Principal Component Analysis (PCA) [12], whose output is essentially the appropriate  $4 \times 4$  rotation matrix, henceforth denoted by  $R$ . Crucially,  $R$  must at bottom function as a model of how points of coordinates  $U, V, W, G$  should be transformed to acquire uncorrelated coordinates. As such, it must take into account as much high-quality data as can be obtained. This holds also for the desired four-dimensional straight line, which can be obtained by a further, restricted use of PCA.

We proceed by first describing how we acquired and processed all the necessary data in Section 2, then presenting results in Section 3. Concluding remarks follow in Section 4.

## 2 Data acquisition and processing

We focus on the accounts of BPMG membership given in [4] and in [13]. The former of these predates the availability of data from the *Gaia* mission. The latter, in turn, is based on an update of the methodology of [5] to contemplate data from *Gaia* DR2. Owing to this, and to the selection criterion used in [13]—only objects to which the model in [5] ascribes a probability greater than 0.9 are admitted—our set of bona fide members is taken from the resulting list.

At a certain point in [4], the search for BPMG members narrows down to a list of 104 candidate members. Of these, 26 were members already known from the literature, 41 turned out to be new members, and 37 were rejected. The 26 known members appear in a final list, along with additional members also known from the literature that did not make the candidate list, amounting to a total of 146. The 41 new members constitute a list of their own. Our versions of these two lists are given in Tables A.1 and A.2, containing respectively the 146 known members and the 41 new members. These two tables contain information obtained during our own process of data acquisition.

The BPMG membership accounted for in [13] contains 64 objects, of which 48 already appear in Table A.1, 5 in Table A.2, and the remaining 11 are given separately in Table A.3. Those already in Table A.1 or Table A.2 are marked with asterisks. Whenever needed, we henceforth refer to the corresponding sub-tables as Table A.1(\*) and Table A.2(\*).

**Data acquisition.** All our data were acquired from the SIMBAD astronomical database (<http://simbad.u-strasbg.fr>) in two separate downloads, both on March 29, 2022, with minor adjustments occurring in the following weeks. Our data, therefore, already contain those that *Gaia* EDR3 made available.

The first download targeted the 198 objects in Tables A.1–A.3, retrieving for each one: right ascension and declination ( $\alpha, \delta$ ) and their quality, proper motion in right ascension and in declination ( $\mu_\alpha, \mu_\delta$ ) and their quality, parallax ( $\pi$ ) and its quality, radial velocity ( $\rho$ ) and its quality,  $G$  and its quality. Each quality is either one of A through E (highest to lowest) or –, the latter indicating that the corresponding data are missing. A tally of this download is shown in Table 1 in regard to data completeness and quality (AAAAC indicates that the spatial and

Table 1: BPMG membership as considered in [4] (known members, cf. Table A.1; new members, cf. Table A.2) or in [13] but not already in [4], cf. Table A.3.

Data availability and quality	Table A.1	Table A.2	Table A.3	Total
Complete data, AAAAC	81	18	5	104
Complete data, others	32	20	6	58
Complete data (total)	113	38	11	162
Incomplete data	33	3	0	36
Grand total	146	41	11	198

Table 2: Object counts in the data set used.

Data availability and quality	BPMG, cf. Table 1			Other objects	Total
	Table A.1	Table A.2	Table A.3		
Complete data, AAAAC	81	18	5	1 586 324	1 586 428
Complete data, others	32	20	6	0	58
Complete data (total)	113	38	11	1 586 324	1 586 486

kinematic data are all of quality A while  $G$  is of quality C, which incidentally is the only quality we ever obtained for  $G$ , not only in this download but in the second one as well). Note that all 36 objects in this download for which data were found to be incomplete serve no purpose in this work. Only the remaining 162 matter.

The second download expanded on the first by targeting a considerably larger body of objects, aiming to put together as many quality-AAAAC objects of appropriate type as available in the database. As such, it necessarily retrieved the 104 quality-AAAAC objects already retrieved in the first download, so duplicates had to be discarded when putting together the quality-AAAAC portion of the final data set. As anticipated in Section 1, the intended use of the data in this second download was to feed the determination of matrix  $R$ . The following SIMBAD object classification types were used in the queries: 10.12.00.00 (Possible peculiar star) and subtypes, 12.13.00.00 (Double or multiple star) and subtypes, 14.00.00.00 (Star) and subtypes. (In SIMBAD query notation, these can all be retrieved by specifying `maintypes = 12.13.00.00` and `maintypes = 14.00.00.00` only.) The result of this download is summarized in the first row of Table 2, whose second row is brought in directly from Table 1. Table 2, therefore, summarizes the totality of all objects used in this work.

**Data processing.** The first processing step of all the data summarized in Table 2 was to obtain  $U$ ,  $V$ , and  $W$  for each object. This was achieved through the usual transformations [14], using the J2000.0 reference system, and was followed by a second step, comprising two runs of PCA after standardization of the data.

For processing by PCA the data must be arranged as an  $n \times p$  matrix  $X$ , where  $p$  is the data set's number of dimensions and  $n$  is the number of  $p$ -dimensional data points. The essence of PCA is the calculation of a  $p \times p$  rotation matrix  $R$  from the covariance matrix of the columns of  $X$  and then using it to project the  $n$  data points onto  $p$  new orthogonal directions, yielding the rotated matrix  $XR$ . The row- $i$ , column- $k$  element of  $XR$  is the so-called  $k$ th principal component (PC  $k$ ) of the  $i$ th data point. Thus, in the present context of  $p = 4$ , the standardized  $U, V, W, G$  get combined into PC 1 through PC 4. Unlike the columns of  $X$ , those of  $XR$  are uncorrelated with one another, and moreover PC 1 explains more of the variance in the data than does PC 2, this one more than PC 3, etc. These two properties justify the typical use of PCA (which is dimensionality reduction), but here we exploit them differently: uncorrelatedness is used to afford better visual exploration; the variance-wise primacy of PC 1, in turn, is used in the determination of the PC-space version of the four-dimensional straight line that seems to bind BPMG members together.

The first PCA run operated on all quality-AAAAC objects accounted for in Table 2, therefore with  $n = 1\,586\,428$ . The resulting  $R$  can be viewed as a model, learned from high-quality data, of how to project standardized  $U, V, W, G$  points onto PC space.

The 41 quality-AAAAC objects in Tables A.1(\*), A.2(\*), and A.3 were then taken to constitute our set of bona fide members. The 121 remaining objects in Tables A.1, A.2, and A.3 with complete data were taken as candidate members. The bona fide members' projections onto PC space were collected in a new  $n \times p$  data matrix, now denoted by  $X'$  and with  $n = 41$ , and used as the basis for the second PCA run. This second run did not aim another rotation of the  $n$  data points, but merely the determination of the best orthogonal fit of a four-dimensional straight line to them. Letting  $\boldsymbol{\mu} = (\mu_1, \dots, \mu_4)$  be the means vector of the  $n$  points, this was achieved by first subtracting  $\boldsymbol{\mu}$  off each row of  $X'$ , then running PCA to determine the new rotation matrix  $R'$ . Let  $\mathbf{a}_1$  be the first column of  $R'$ , that is, the vector to which the first component (now called PC 1') of the data in  $X'$  refers. In parametric form, and for  $-\infty < t < \infty$ , the straight line going through  $\boldsymbol{\mu}$  in the direction of  $\mathbf{a}_1$  is  $\mathbf{f}(t) = \boldsymbol{\mu} + t\mathbf{a}_1$ . Because PC 1' accounts for more variance in  $X'$  than any of the other three principal components,  $\mathbf{f}(t)$  is the straight line to which all  $n$  points are closest in the least-squares sense and is therefore the desired four-dimensional straight line. We henceforth view  $\mathbf{f}(t)$  as a linear model of the BPMG and refer to it simply as PC 1'.

### 3 Results

Our results are summarized as the two-dimensional plots in the six panels of Figure 1. Each panel zooms in on a different two-dimensional projection of the data set of Table 2 after standardization and rotation, with the quality-AAAAC "Other objects" represented as tiny dots in the background and the bona fide and candidate members as larger, color-coded dots in the foreground. It must

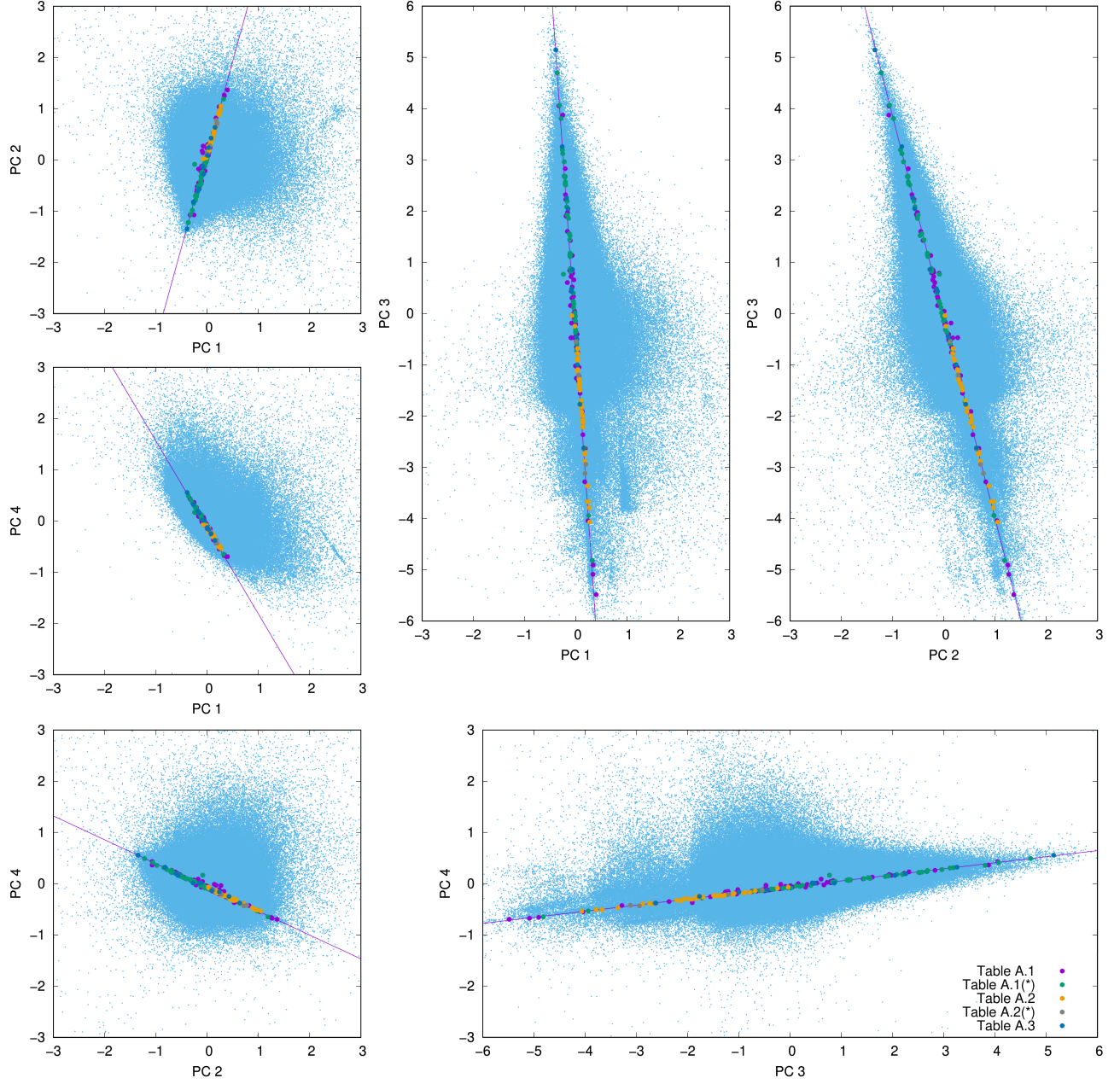


Figure 1: Two-dimensional projections of the full data set of Table 2 after standardization and rotation, for all six pairs of distinct principal-component axes. The straight line PC 1' is projected as well.

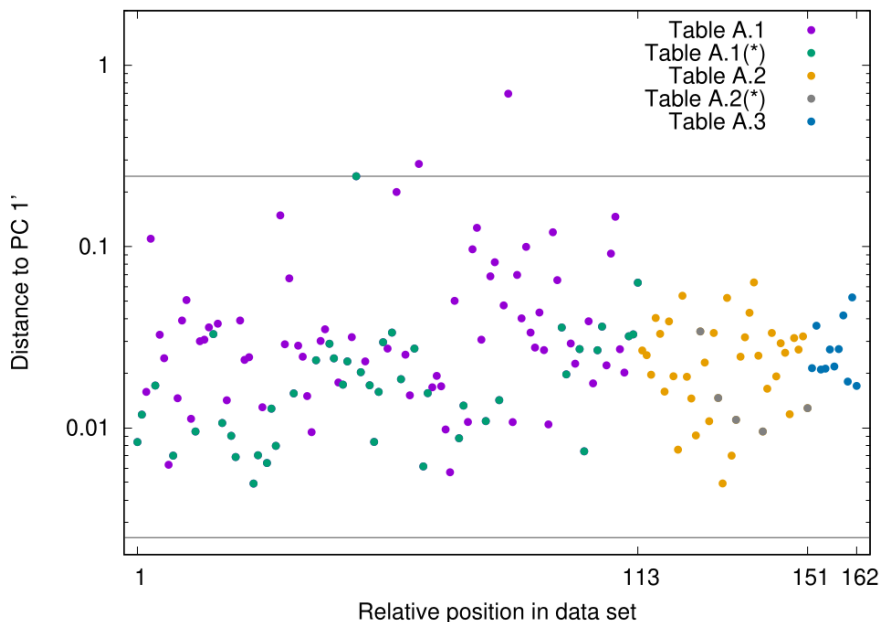


Figure 2: Distances to PC 1' for the BPMG objects in Table 2. The horizontal gray lines mark the lower and upper thresholds (about 0.002 and 0.244) for outlier flagging.

be noted that the latter include both the 104 quality-AAAAC objects and the remaining 58, lower-quality ones. (One technicality is that these 58 objects had to undergo the same standardization as the others before rotation, being altered by means and standard deviations in which they did not participate.) Visible in all panels is the corresponding projection of PC 1' as well.

While the plots in Figure 1 seem to suggest a great proximity of the bona fide members to PC 1', to varying degrees this can also be said of the candidate members. A better view of these distances for all 162 objects of Table 2 is given in Figure 2. Not only does this figure show that distances are in fact spread more widely than we might suppose by simply examining Figure 1, it tellingly also reveals that some of those objects do indeed lie farther apart from PC 1' than do the bona fide ones or those that lie, so to speak, in their ballpark. It then makes sense that we should try and set aside the ones that would be flagged as outliers by some criterion. Most such criteria assume the data to follow a normal distribution, though testing them for this is inevitably affected by the presence of the very outliers to be eventually flagged.

Distances to PC 1' are definitely not normally distributed, but visually inspecting the distribution of their natural logarithms does change this significantly, as illustrated in Figure 3. That is, the distances themselves seem to follow an approximately lognormal distribution. Even this is far from fully

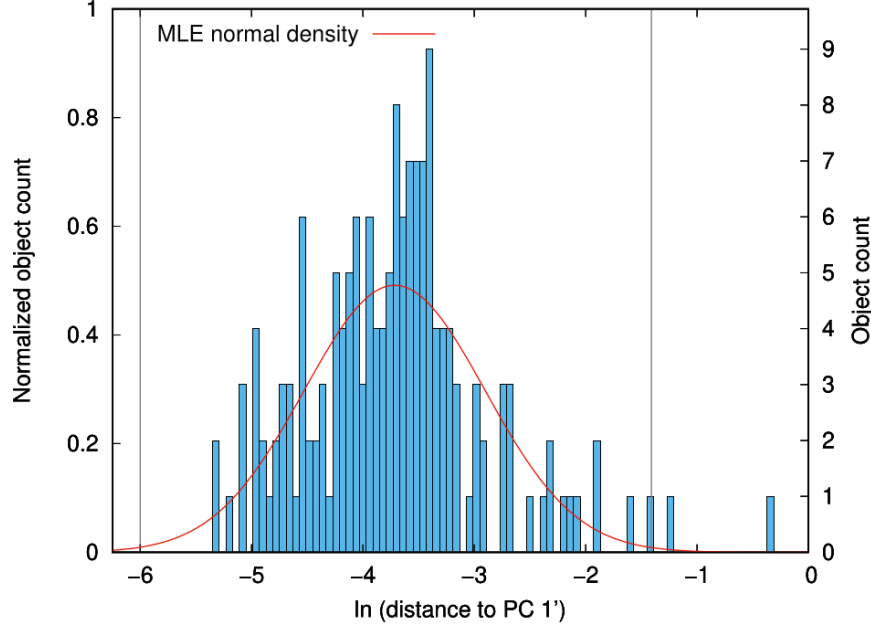


Figure 3: Normalized histogram and MLE normal density of the natural logarithms of distances to PC 1' for the BPMG objects in Table 2. The corresponding original object counts are given on the vertical axis on the right for context. The vertical gray lines mark the lower and upper thresholds (about  $-6$  and  $-1.41$ ) for outlier flagging.

reliable, though, as the MLE (maximum-likelihood estimate) normal density plotted in the same figure suggests. In cases such as this, customarily one resorts to outlier-flagging methods that substitute the median for the mean and the MAD (median absolute deviation) for the standard deviation. In general this provides some added robustness in the face of uncertain normality of the data.

A widely used method that does this is the modified Z-score method [15]. For  $\ln(\mathbf{d})$  denoting the vector with the natural logarithms of all 162 distances to PC 1' and  $\ln(d_i)$  its  $i$ th element, this method's recommendation is to flag the  $i$ th object as an outlier worthy of further investigation if

$$|\ln(d_i) - \text{median}(\ln(\mathbf{d}))| > \frac{3.5 \text{ median}(|\ln(d_k) - \text{median}(\ln(\mathbf{d}))|)}{0.6745}. \quad (1)$$

In this expression, the range of  $k$  is all of  $\ln(\mathbf{d})$ . For  $\ln(d_i) < \text{median}(\ln(\mathbf{d}))$ , the equation above leads to a threshold of about  $-6$ , below which flagging is recommended (that is, approximately for distances below  $e^{-6} \approx 0.002$ ). For  $\ln(d_i) > \text{median}(\ln(\mathbf{d}))$ , a threshold of about  $-1.41$  is obtained, above which flagging is recommended as well (that is, approximately for distances above



Table 3: Possible outliers relative to distances to PC 1'.

2MASS J	SIMBAD (main identifier)	Data quality						Distance to PC 1'
		$\alpha, \delta$	$\mu_\alpha, \mu_\delta$	$\pi$	$\rho$	$G$		
00325584-4405058	EROS-MP J0032-4405	A	A	A	B	C	0.696	
20135152-2806020	2MASS J20135152-2806020	A	A	A	A	C	0.285	

$e^{-1.41} \approx 0.244$ ). These thresholds are marked both as horizontal gray lines in Figure 2 and as vertical gray lines in Figure 3, setting apart no objects lying strictly below the lower threshold and only two lying strictly above the upper threshold. These possible outliers are brought in from Table A.1 and listed in Table 3 in decreasing order of distance to PC 1'.

Except for  $\rho$ , the currently available spatial and kinematic data for the two possible outliers listed in Table 3 (and to which the quality indicators in the table refer) all come from *Gaia* EDR3. These two objects, however, were included as known BPMG members in [4] from earlier literature, therefore prior to the availability of any data from the *Gaia* mission. 2MASS J00325584-4405058 was brought in from [16], where it is listed as a candidate member despite the absence of a reliable  $\rho$  measurement. It was moreover not tested by the proposed selection process in [4], having therefore undergone no further confirmation. 2MASS J20135152-2806020, in turn, is from [17], where the authors caution that membership confirmation depends on further verification, “typically with radial velocity measurements.” It passed the test in [4], based in part on  $\rho = -5.81 \pm 0.5 \text{ km s}^{-1}$ , which seems to agree with the current best estimate ( $\rho = -6.53 \pm 0.24 \text{ km s}^{-1}$ , cf. [18]) only by the thinnest margin.

It must also be noted that, though not listed as a possible outlier in Table 3, 2MASS J18141047-3247344 (HD 319139, a binary system hosting a protoplanetary disk), the third farthest object from PC 1', misses the upper threshold by only a hair's breadth. It too was brought into [4] from elsewhere [9] and passed the authors' selection process. However, this seems to have taken into account  $\rho = -13.3 \pm 7.7 \text{ km s}^{-1}$  while the best estimate now available is markedly different ( $\rho = -51.01 \pm 0.59 \text{ km s}^{-1}$ , cf. [19]). This notwithstanding, this object's absence from Table 3 is of course amply supported by its presence amid our bona fide members, which we recall comprises only quality-AAAAC objects in the list from [13]; cf. Table A.1(\*). In any event, it seems advisable to keep monitoring the measurements of  $\rho$  for this object.

## 4 Concluding remarks

Deciding on an object's membership status in the BPMG (and, in general, in any other young stellar moving group) must rely on the measurement of several astrophysical properties that can be hard and expensive to acquire. In this work we have introduced a new tool that can be used in the process. At the heart of this tool is PCA, one of the staple techniques in data science, here used for its ability to rotate variables so they become uncorrelated and to automatically

identify the one resulting variable to which more variance in the data can be ascribed than to any other. The outcome of interest is the four-dimensional straight line we have called PC 1'.

In the case of the BPMG, we demonstrated that PC 1' can function as a linear model of the group, since distances from candidate members to it can be used as a kind of proxy for group membership. We reached this conclusion by partitioning the membership compilation of [13] into a set of bona fide members and a set of candidate members, and then enlarging the latter set with the inclusion of several objects from the compilation of [4]. PC 1' was constructed from the set of bona fide members, using further quality-AAAAC data on more than 1.5 million objects. For the case of the BPMG these data were ultimately standardized versions of  $U, V, W, G$ , but alternatives can certainly be considered. Of course, one downside of the overall approach is that complete data are needed for all participating objects, but again obtaining such data is a constantly pursued goal. In general, it is a matter of time before they become available.

## Acknowledgments

We thank Vladimir G. Ortega for introducing us to the topic of the BPMG and Joel Kastner for commenting on an earlier version. We acknowledge partial support from Conselho Nacional de Desenvolvimento Científico e Tecnológico (CNPq), Coordenação de Aperfeiçoamento de Pessoal de Nível Superior (CAPES), and a BBP grant from Fundação Carlos Chagas Filho de Amparo à Pesquisa do Estado do Rio de Janeiro (FAPERJ).

## References

- [1] B. Zuckerman, I. Song, M. S. Bessell, and R. A. Webb. The  $\beta$  Pictoris moving group. *Astrophys. J.*, 562:L87–L90, 2001.
- [2] A.-M. Lagrange, M. Bonnefoy, G. Chauvin, D. Apai, D. Ehrenreich, A. Boccaletti, D. Gratadour, D. Rouan, D. Mouillet, S. Lacour, and M. Kasper. A giant planet imaged in the disk of the young star  $\beta$  Pictoris. *Science*, 329:57–59, 2010.
- [3] A.-M. Lagrange, N. Meunier, P. Rubini, M. Keppler, F. Galland, E. Chapellier, E. Michel, L. Balona, H. Beust, T. Guillot, A. Grandjean, S. Borgniet, D. Mékarnia, P. A. Wilson, F. Kiefer, M. Bonnefoy, J. Lillo-Box, B. Pantoja, M. Jones, D. P. Iglesias, L. Rodet, M. Diaz, A. Zapata, L. Abe, and F.-X. Schmider. Evidence for an additional planet in the  $\beta$  Pictoris system. *Nat. Astron.*, 3:1135–1142, 2019.
- [4] E. L. Shkolnik, K. N. Allers, A. L. Kraus, M. C. Liu, and L. Flagg. All-sky Co-moving Recovery Of Nearby Young Members (ACRONYM). II. The  $\beta$  Pictoris moving group. *Astron. J.*, 154:69, 2017.

- [5] J. Gagné, E. E. Mamajek, L. Malo, A. Riedel, D. Rodriguez, D. Lafrenière, J. K. Faherty, O. Roy-Loubier, L. Pueyo, A. C. Robin, and R. Doyon. BANYAN. XI. The BANYAN  $\Sigma$  multivariate Bayesian algorithm to identify members of young associations with 150 pc. *Astrophys. J.*, 856:23, 2018.
- [6] J. Lee and I. Song. Evaluation of nearby young moving groups based on unsupervised machine learning. *Mon. Not. R. Astron. Soc.*, 489:2189–2194, 2019.
- [7] B. Zuckerman and I. Song. Young stars near the Sun. *Annu. Rev. Astron. Astrophys.*, 42:685–721, 2004.
- [8] C. A. O. Torres, G. R. Quast, L. da Silva, R. de la Reza, C. H. F. Melo, and M. Sterzik. Search for associations containing young stars (SACY). I. Sample and searching method. *Astron. Astrophys.*, 460:695–708, 2006.
- [9] C. A. O. Torres, G. R. Quast, C. H. F. Melo, and M. F. Sterzik. Young nearby loose associations. In B. Reipurth, editor, *Handbook of Star Forming Regions, Volume II: The Southern Sky*, pages 757–812. Astronomical Society of the Pacific, San Francisco, CA, 2008.
- [10] V. Estivill-Castro. Why so many clustering algorithms—A position paper. *SIGKDD Explor.*, 4:65–75, 2002.
- [11] M. Weiler. Revised *Gaia* Data Release 2 passbands. *Astron. Astrophys.*, 617:A138, 2018.
- [12] I. T. Jolliffe and J. Cadima. Principal component analysis: a review and recent developments. *Philos. Trans. R. Soc. A*, 374:20150202, 2016.
- [13] A. L. Carter, S. Hinkley, M. Bonavita, M. W. Phillips, J. H. Girard, M. Perrin, L. Pueyo, A. Vigan, J. Gagné, and A. J. I. Skemer. Direct imaging of sub-Jupiter mass exoplanets with *James Webb Space Telescope* coronagraphy. *Mon. Not. R. Astron. Soc.*, 501:1999–2016, 2021.
- [14] D. R. H. Johnson and D. R. Soderblom. Calculating galactic space velocities and their uncertainties, with an application to the Ursa Major Group. *Astron. J.*, 93:864–867, 1987.
- [15] B. Iglewicz and D. Hoaglin. *How to Detect and Handle Outliers*, volume 16 of *The ASQC Basic References in Quality Control: Statistical Techniques*. ASQC Quality Press, Milwaukee, WI, 1993.
- [16] J. Gagné, D. Lafrenière, R. Doyon, L. Malo, and É. Artigau. BANYAN. V. A systematic all-sky survey for new very late-type low-mass stars and brown dwarfs in nearby young moving groups. *Astrophys. J.*, 798:73, 2015.
- [17] M. C. Liu, T. J. Dupuy, and K. N. Allers. The Hawaii Infrared Parallax Program. II. Young ultracool field dwarfs. *Astrophys. J.*, 833:96, 2016.

- [18] J. K. Faherty, A. R. Riedel, K. L. Cruz, J. Gagné, J. C. Filippazzo, E. Lambrides, H. Fica, A. Weinberger, J. R. Thorstensen, C. G. Tinney, and V. Baldassare. Population properties of brown dwarf analogs to exoplanets. *Astrophys. J. Suppl. Ser.*, 225:10, 2016.
- [19] N. Miret-Roig, P. A. B. Galli, W. Brandner, H. Bouy, D. Barrado, J. Olivares, T. Antoja, M. Romero-Gómez, F. Figueras, and J. Lillo-Box. Dynamical traceback age of the  $\beta$  Pictoris moving group. *Astron. Astrophys.*, 642:A179, 2020.

## A Supplementary tables

This appendix contains Tables A.1–A.3.

Table A.1: Identifiers and data quality of the BPMG members listed in Table 4 (first part, known members) of [4].

2MASS J	Also in [13]	SIMBAD (main identifier)	Data quality				
			$\alpha, \delta$	$\mu_\alpha, \mu_\delta$	$\pi$	$\rho$	$G$
00065008-2306271	*	HD 203	A	A	A	C	C
00172353-6645124	*	SCR J0017-6645	A	A	A	A	C
00233468+2014282		V* FK Psc	B	B	-	A	-
00274534-0806046		SCR J0027-0806	A	A	A	B	C
00275023-3233060	*	GJ 2006 A	A	A	A	A	C
00275035-3233238		GJ 2006 B	A	A	A	A	C
00325584-4405058		EROS-MP J0032-4405	A	A	A	B	C
00440332+0228112		2MASS J00440332+0228112	C	D	-	-	-
00464841+0715177		2MASS J00464841+0715177	A	A	A	A	C
01071194-1935359		RX J0107.1-1935	B	B	-	A	C
01112542+1526214		LP 467-16	B	C	D	A	C
01132817-3821024		CD-39 325	B	C	-	A	-
01294256-0823580		2MASS J01294256-0823580	A	A	A	-	C
01351393-0712517	*	Barta 161 12	A	A	A	A	C
01354915-0753470		GPM 23.953841-07.895919	A	A	A	C	C
01365516-0647379		G 271-110	A	A	A	A	C
01373545-0645375		V* EX Cet	A	A	A	A	C
01373940+1835332	*	BD+17 232	B	B	-	A	-
01535076-1459503		RX J0153.5-1459	B	C	-	A	-
02172472+2844305		HD 14082B	A	A	A	A	C
02172527+2844423	*	HD 14082	A	A	A	A	C
02175601+1225266		PM J02179+1225	A	A	A	A	C
02232663+2244069		LP 353-51	A	A	A	A	C
02261625+0617331		HD 15115	A	A	A	A	C
02272804+3058405		BD+30 397B	A	A	A	A	C
02272924+3058246	*	BD+30 397	A	A	A	A	C

Table A.1: Continued.

2MASS J	Also in [13]	SIMBAD (main identifier)	Data quality				
			$\alpha, \delta$	$\mu_\alpha, \mu_\delta$	$\pi$	$\rho$	$G$
02282694+0218331		2MASS J02282694+0218331	A	A	A	-	C
02303239-4342232		CD-44 753	A	A	A	A	C
02304623-4343493		UCAC2 13050114	A	A	A	A	C
02365171-5203036		EXO 0235.2-5216	A	A	A	B	C
02412589+0559181		BD+05 378	A	A	A	A	C
02501167-0151295		TVLM 831-154910	A	A	A	-	C
02534448-7959133		SIPS J0253-7959	A	A	A	-	C
03111547+0106307		[BHR2005] 832-2	A	A	A	D	C
03323578+2843554		RX J0332.6+2843	B	C	-	A	C
03350208+2342356	*	2MASSW J0335020+234235	A	A	A	B	C
04373613-0228248	*	* 51 Eri	A	A	A	A	C
04373746-0229282		StKM 1-497	A	A	A	A	C
04433761+0002051	*	2MASSI J0443376+000205	A	A	A	A	C
04435686+3723033		V* V962 Per	A	A	A	A	C
04480085+1439583		UCAC2 36944937	A	A	A	-	C
04480258+1439516		UCAC3 210-20333	A	A	A	-	C
04593483+0147007	*	V* V1005 Ori	A	A	A	A	C
05004714-5715255	*	CD-57 1054	A	A	A	A	C
05015881+0958587	*	LP 476-207	A	A	A	B	-
05082729-2101444		UCAC4 345-006842	A	A	A	A	C
05120636-2949540		2MASS J05120636-2949540	C	C	-	-	C
05195327+0617258		GSC2.3 N9OB003170	A	A	A	-	C
05200029+0613036		RX J0520.0+0612	A	A	A	A	C
05203182+0616115		RX J0520.5+0616	A	A	A	A	C
05241914-1601153		PM J05243-1601	B	C	-	A	-
05270477-1154033	*	V* AF Lep	A	A	A	A	C
05294468-3239141	*	RX J0529.7-3239	A	A	A	A	C
05335981-0221325		RX J0534.0-0221	A	A	A	A	C
05471708-5103594	*	* bet Pic	A	A	A	A	C
06131330-2742054	*	RX J0613.2-2742	A	A	A	A	C
06182824-7202416	*	V* AO Men	A	A	A	A	C
08173943-8243298		1RXS J081742.4-824331	A	A	A	B	C
08224744-5726530		L 186-67	A	A	A	A	C
09360429+3733104		HD 82939	A	A	A	A	C
09361593+3731456		MCC 549	A	A	A	D	C
10141918+2104297		MCC 124	A	A	A	A	C
10172689-5354265	*	TWA 22	A	A	A	A	C
10593834+2526155		HD 95174A	A	A	A	A	C
10593870+2526138		HD 95174B	A	A	A	D	C
11493184-7851011		V* DZ Cha	A	A	A	A	C

Table A.1: Continued.

2MASS J	Also in [13]	SIMBAD (main identifier)	Data quality				
			$\alpha, \delta$	$\mu_\alpha, \mu_\delta$	$\pi$	$\rho$	$G$
13545390-7121476		UPM J1354-7121	A	A	A	A	C
14141700-1521125		L 836-122	A	A	A	-	C
14142141-1521215		HD 124498	A	A	A	A	-
14252913-4113323		SCR J1425-4113AB	A	A	A	B	C
15385679-5742190		HD 139084B	A	A	A	A	C
15385757-5742273	*	HD 139084	A	A	A	A	C
16181789-2836502		* d Sco	A	A	A	A	C
16430128-1754274		ASAS J164301-1754.4	A	A	A	A	C
16572029-5343316	*	TYC 8726-1327-1	A	A	A	A	C
17150219-3333398		1RXS J171502.4-333344	A	A	A	C	C
17150362-2749397		CD-27 11535	A	A	A	C	C
17172550-6657039	*	HD 155555	A	A	A	A	C
17173128-6657055		HD 155555C	A	A	A	A	C
17292067-5014529		GSC 08350-01924	C	D	-	B	-
17295506-5415487	*	CD-54 7336	A	A	A	A	C
17414903-5043279	*	HD 160305	A	A	A	C	C
17483374-5306433	*	HD 161460	A	A	A	C	C
18030341-5138564	*	HD 164249	A	A	A	A	C
18030409-5138561		HD 164249B	A	A	A	A	C
18064990-4325297	*	CD-43 12272	A	A	A	A	-
18141047-3247344	*	HD 319139	A	A	A	A	C
18142207-3246100		ASAS J181422-3246.2	A	A	A	C	C
18151564-4927472		2MASS J18151564-4927472	A	A	A	C	C
18195221-2916327	*	HD 168210	A	A	A	C	C
18202275-1011131		BD-10 4662	A	A	A	A	-
18420483-5554126	*	UCAC4 171-199133	A	A	A	A	C
18420694-5554254		1RXS J184206.5-555426	A	A	A	A	C
18452691-6452165	*	HD 172555	A	A	A	C	C
18453704-6451460		CD-64 1208	A	A	A	C	C
18465255-6210366		Smethells 20	A	A	A	C	C
18480637-6213470	*	HD 173167	A	A	A	A	C
18504448-3147472	*	CD-31 16041	A	A	A	C	C
18530587-5010499	*	V* PZ Tel	A	A	A	A	C
18580415-2953045	*	1RXS J185803.4-295318	A	A	A	C	C
18580464-2953320		UCAC2 19527490	C	B	-	A	C
19102820-2319486		1SWASP J191028.18-231948.0	C	-	-	A	C
19114467-2604085		CD-26 13904	A	A	A	C	C
19225122-5425263		* eta Tel	A	A	A	C	C
19225894-5432170	*	HD 181327	A	A	A	A	C
19233820-4606316	*	ASAS J192338-4606.4	A	A	A	A	C

Table A.1: Continued.

2MASS J	Also in [13]	SIMBAD (main identifier)	Data quality				
			$\alpha, \delta$	$\mu_\alpha, \mu_\delta$	$\pi$	$\rho$	$G$
19243494-3442392		2MASS J19243494-3442392	A	A	A	A	C
19312434-2134226		2MASS J19312434-2134226	A	A	A	B	C
19355595-2846343	*	2MASS J19355595-2846343	A	A	A	A	C
19560294-3207186		UCAC3 116-474938	A	A	A	A	C
19560438-3207376	*	PM J19560-3207	A	A	A	A	C
20004841-7523070		SIPS J2000-7523	A	A	A	B	C
20013718-3313139		UCAC4 284-205440	A	A	A	A	C
20041810-2619461		HD 190102	A	A	A	A	C
20055640-3216591		V* V5663 Sgr	A	A	A	B	C
20090521-2613265	*	HD 191089	A	A	A	A	C
20100002-2801410		SCR J2010-2801	B	C	-	A	C
20135152-2806020		2MASS J20135152-2806020	A	A	A	A	C
20333759-2556521	*	SCR J2033-2556	A	A	A	A	C
20334670-3733443		SIPS J2033-3733	A	A	A	-	C
20415111-3226073		V* AT Mic	A	A	A	A	-
20434114-2433534	*	EM* StHA 182	B	C	-	A	-
20450949-3120266	*	V* AU Mic	A	A	A	A	C
20554767-1706509	*	HD 199143	A	A	A	C	C
20560274-1710538		HD 358623	B	C	D	A	-
21100461-1920302	*	UCAC4 354-189365	A	A	A	B	C
21100535-1919573		BPS CS 22898-0065	A	A	A	A	C
21103096-2710513		2MASS J21103096-2710513	A	A	A	A	C
21103147-2710578		** BRG 32A	A	A	A	A	C
21140802-2251358		2MASS J21140802-2251358	C	C	C	-	-
21212446-6654573		V* V390 Pav	A	A	A	E	C
21212873-6655063		PM J21214-6655	A	A	A	A	C
21374019+0137137		RX J2137.6+0137	A	A	A	A	C
22004158+2715135		RX J2200.7+2715	A	A	A	A	C
22081363+2921215		2MASSW J2208136+292121	C	C	C	B	-
22424896-7142211	*	CPD-72 2713	A	A	A	A	C
22445794-3315015	*	V* WW PsA	A	A	A	A	C
22450004-3315258		V* TX PsA	A	A	A	A	C
23172807+1936469		G 68-5	A	A	A	A	C
23301341-2023271		G 273-59	A	A	A	A	C
23314492-0244395		V* AF Psc	A	A	A	A	C
23323085-1215513	*	BPM 82931	A	A	A	A	C
23353085-1908389		2MASS J23353085-1908389	A	A	A	-	C
23500639+2659519		RX J2350.0+2659	A	A	A	A	C
23512227+2344207		G 68-46	A	A	A	A	C
23542220-0811289		2MASS J23542220-0811289	C	D	-	-	-

Table A.2: Identifiers and data quality of the BPMG members listed in Table 4 (second part, new members) of [4].

2MASS J	Also in [13]	SIMBAD (main identifier)	Data quality				
			$\alpha, \delta$	$\mu_\alpha, \mu_\delta$	$\pi$	$\rho$	$G$
00164976+4515417		2MASS J00164976+4515417	C	E	-	A	-
00193931+1951050		2MASS J00193931+1951050	A	A	A	A	C
00194303+1951117		RX J0019.7+1951	A	A	A	A	C
00281434-3227556		GR* 9	A	A	A	C	C
00413538-5621127		DENIS J004135.3-562112	A	A	A	B	C
00482667-1847204		2MASS J00482667-1847204	A	A	A	A	C
00501752+0837341		PM J00502+0837	A	A	A	B	C
01303534+2008393		2MASS J01303534+2008393	A	A	A	A	C
02241739+2031513	*	2MASS J02241739+2031513	A	A	A	B	C
02335984-1811525		RX J0234.0-1811	B	C	-	A	-
02450826-0708120		2MASS J02450826-0708120	A	A	A	C	C
02485260-3404246		UCAC3 112-6119	A	A	A	A	C
02495639-0557352		2MASS J02495639-0557352	A	A	A	A	C
03255277-3601161		UCAC2 16305530	A	A	A	C	C
03363144-2619578		SCR J0336-2619	A	A	A	C	C
03370343-3042318		2MASS J03370343-3042318	A	A	A	C	C
03393700+4531160		PM J03396+4531	A	A	A	B	C
03550477-1032415		2MASS J03550477-1032415	A	A	A	A	C
04232720+1115174		2MASS J04232720+1115174	A	A	A	A	C
05015665+0108429		PM J05019+0108	A	A	A	A	C
05061292+0439272	*	RX J0506.2+0439	A	A	A	C	C
05363846+1117487		PM J05366+1117	A	A	A	A	C
13215631-1052098		PM J13219-1052	A	A	A	C	C
15063505-3639297		2MASS J15063505-3639297	A	A	A	B	C
18011345+0948379		UPM J1801+0948	A	A	A	B	C
18055491-5704307		UPM J1805-5704	A	A	A	A	C
18090694-7613239		SIPS J1809-7613	A	A	A	A	C
18092970-5430532		2MASS J18092970-5430532	A	A	A	A	C
18435838-3559096		2MASS J18435838-3559096	A	A	A	C	C
18471351-2808558		2MASS J18471351-2808558	A	A	A	B	C
19082195-1603249	*	2MASS J19082195-1603249	A	A	A	A	C
19260075-5331269		2MASS J19260075-5331269	A	A	A	C	C
19300396-2939322		2MASS J19300396-2939322	A	A	A	B	C
20083784-2545256		2MASS J20083784-2545256	A	A	A	B	C
20085368-3519486		UCAC4 274-196167	B	C	-	A	-
21200779-1645475		2MASS J21200779-1645475	A	A	A	A	C
21384755+0504518		2MASS J21384755+0504518	A	A	A	B	C
22085034+1144131	*	PM J22088+1144	A	A	A	B	C
22334687-2950101		2MASS J22334687-2950101	A	A	A	A	C
23010610+4002360		2MASS J23010610+4002360	A	A	A	A	C
23355015-3401477	*	SIPS J2335-3401	A	A	A	A	C



Table A.3: Identifiers and data quality of the BPMG members listed in Table A1 of [13], excluding those already appearing in Table A.1 or Table A.2, where they are marked with asterisks.

2MASS J	SIMBAD (main identifier)	Data quality				
		$\alpha, \delta$	$\mu_\alpha, \mu_\delta$	$\pi$	$\rho$	$G$
05004928+1527006	HD 286264	A	A	A	A	C
05315786-0303367	PM J05319-0303W	A	A	A	B	C
05320450-0305291	V* V1311 Ori	A	A	A	A	C
05320596-0301159	ESO-HA 737	A	A	A	C	C
14423039-6458305	* alf Cir	A	A	A	A	C
17453733-2824269	HD 161247	A	A	A	C	C
17520173-2357571	PM J17520-2357	A	A	A	B	C
18183181-3503026	HD 167847B	A	A	A	C	C
20524162-5316243	HD 198472	A	A	A	A	C
21354554-4218343	[HB88] M11	A	A	A	B	C
22311828-0633183	HD 213429	A	A	A	A	C